Behavioral/Systems/Cognitive

Central V4 Receptive Fields Are Scaled by the V1 Cortical Magnification and Correspond to a Constant-Sized Sampling of the V1 Surface

Brad C. Motter

Veterans Affairs Medical Center, Syracuse, New York 13210, and Department of Neuroscience and Physiology, State University of New York Upstate Medical University, Syracuse, New York 13210

The mapping of the topographic representation of the visual field onto cortical areas changes throughout the hierarchy of cortical visual areas. The changes are believed to reflect the establishment of modules with different spatial processing emphasis. The receptive fields (RFs) of neurons within these modules, however, may not be governed by the same spatial topographic map parameters. Here it is shown that the RFs of area V4 neurons (centered 1–12° in eccentricity) are based on a circularly symmetric sampling of the primary visual cortical retinotopic map. No eccentricity dependent magnification beyond that observed in V1 is apparent in the V4 neurons. The size and shape of V4 RFs can be explained by a simple, constant sized, two-dimensional Gaussian sample of visual input from the retinotopic map laid out across the surface of V1. Inferences about the spatial scale of interactions within the receptive fields of neurons cannot be based on a visual area's apparent cortical magnification derived from topographic mapping.

Introduction

As information disperses from primary visual cortex throughout the cortical visual areas there are differential expansions of the spatial representation of the central compared with the peripheral visual fields. The expansion of the visual field as defined in topographic maps differs in the visual streams directed toward temporal versus parietal lobe visual areas in a manner that parallels the differences in information processing in those areas. There is an emphasis on foveal representation in temporal areas and peripheral representation in parietal areas (for review, see Gattass et al., 2005). However, a fundamental linkage between the anisotropies (including cortical magnification) of topographic visual field maps and the structure of the individual neuronal receptive fields (RFs) within a cortical area has not been demonstrated.

In our psychophysical studies of visual search we found that target detection is a linear function of the separation between the target and its nearest distractor when distances between those objects are scaled by the cortical magnification factor for area V1 (Motter and Holsapple, 2000, 2001; Motter and Simoni, 2007, 2008). This relationship can be represented as a constant cortical spacing between neural images across the surface of area V1, independent of target eccentricity. Our observations based on perceptual performance place certain constraints on the neural spatial scaling factors that underlie the observed performances. We demonstrated with a mathematical proof that the constraints imply that cortical magnification as a whole must maintain the scaling factor for V1, modified at most by a simple gain, at least to the level of the visual hierarchy where such perceptual performance is determined (Motter and Holsapple, 2000). This constraint on cortical magnification is at odds with the topographic mapping representations and the inferred cortical magnification factors associated with the differential expansion of the representation of the central versus peripheral visual fields in many visual areas beyond primary visual cortex.

The hypothesis put forth here is that changes in the magnification of the visual field map from area to area do not imply changes in the neuronal receptive field structure. We show that the observed asymmetry of central V4 receptive fields results from a simple circularly symmetric, Gaussian sampling of the distorted visual field representation that is laid out across the surface of area V1; thus a circle traced out on the surface of V1 describes a trajectory in visual space that matches the RF edge of V4 neurons. The results imply that with respect to the processing of individual V4 neurons there is no eccentricity dependent magnification change after primary visual cortex; this matches our expectations from the behavioral observations. To visualize the neural and perceptual hypotheses a three-dimensional (3D) model of the V1 surface based on the work of Daniel and Whitteridge (1961) and Rovamo and Virsu (1984) was constructed. The RFs of V4 neurons were projected onto the surface of the model so that the symmetry and spatial relationships could be examined.

Materials and Methods

Data were obtained from four rhesus monkeys, trained and prepared for behavioral neurophysiological recording experiments. Standard electrophysiological techniques were used to obtain recordings from neurons in extrastriate area V4 (Motter, 1994, 2006). The impulse activity of single cortical neurons was recorded with glass-coated Elgiloy microelectrodes inserted transdurally into the cortex. Eye position was measured (400

Received Sept. 18, 2008; revised Feb. 10, 2009; accepted March 26, 2009.

This research was supported by a grant from the Veterans Affairs Bio-Medical Research Program and by National Institutes of Health Grant R01-EY018693.

Correspondence should be addressed to Brad C. Motter, Research Service 151, VA Medical Center, 800 Irving Avenue, Syracuse, NY 13210. E-mail: motterb@cnyrc.org.

DOI:10.1523/JNEUROSCI.4496-08.2009

 0270-6474/09/295749-09$15.00/0

Hz) with a scleral search coil system. All experimental protocols were approved by the animal studies committees at the VA Medical Center and at SUNY Upstate Medical University.

Behavioral paradigms. Monkeys were trained to perform a simple fixation task that required steady fixation of a small spot of light for several seconds while behaviorally irrelevant stimuli were presented in the near periphery up to 20° from fixation. At the end of the trial the fixation spot moved a small distance (<0.75°) in a random direction and the monkey was required to refixate it within a reaction time window to receive a reward. During the fixation task a neuron's receptive field (RF) was mapped and each neuron's response preferences for stimulus shape, size, orientation, and color was determined. The monkeys were required to keep eye position inside a 1° circular window centered on the fixation spot. All stimuli were viewed binocularly. The fixation target was displaced from screen center so as to center the RF on the screen during RF mapping. The animals worked daily for 1200–1500 trials at ~85% correct performance.

Stimulus presentation. Stimuli were generated using custom software and a Number Nine Pepper SGT graphics card. Stimuli were presented on a SONY GDM F520 monitor located at a 57 cm viewing distance. Stimulus timing was synchronized with the vertical refresh of the graphics display system. Each series of stimuli were presented in a pseudorandom sequence. The stimuli consisted of letter-like figures, such as T, I, E, L, F, O, Z or their mirror images presented at various orientations.

Procedures and data analysis. Single neurons were initially selected for study if they responded to flashed stimuli (~2.0 × 0.2°) that were used to activate the neural record during electrode advancement. Computer runs were used to estimate the RF location and preferences for size, color, shape and orientation of stimuli. A significant effort was made to find a combination of parameters that elicited robust responses. From these efforts a preferred stimulus was defined and used to map the RF. V4 RFs were mapped by establishing a 16 by 16 point grid centered on the RF. One axis of the grid was aligned with the orientation preference of the neuron. Stimulus orientation preference was defined by the long axis of the optimal stimulus. If the neuron was not orientation sensitive or if the optimal stimulus was completely symmetric (a circle) then an orientation of 90° (vertical) was used. The spacing of the grid matrix was chosen to encompass the RF at least to the extent possible for the larger eccentric fields. During a series of fixation trials stimuli were rapidly and sequentially flashed at each of the 256 grid locations according to a random permutation sequence. To counter the rapid habituation of V4 responses to sequences of stimuli (Motter, 2006), each stimulus ON period (100 ms) was followed by a blank screen for 100–150 ms. In addition the pseudorandom schedule avoided sequential presentations at nearby locations. Response averages for each grid location were obtained by a reverse correlation technique in which each neural discharge was associated with the stimulus that was present in a preceding temporal interval. The mean response onset latency was 67 ms with an SD of 12 ms. The look-back interval chosen for the reverse correlation analysis maximized the peak response observed at any of the 256 sites. Contour plots of the response rates were made. Receptive field size was calculated by measuring the area bound by the contour enclosing rates >50% of baseline; RF size is reported as the square root of that area.

The complete receptive field maps used for quantitative data analysis were almost exclusively obtained for receptive fields with centers within 12° of the fovea. This limitation was the result of the size of the display monitor and the viewing distance. Additional mappings were made of RFs at larger eccentricities using closer viewing distances, but those results are not used for analysis because of the problems in maintaining retinotopically constant stimuli when using a tangent screen. In addition V4 RFs centered at 25–30° eccentricity often extended beyond the limits of the tangent video display screen. Nevertheless the partial RF maps that were obtained at these greater eccentricities were represented on the V1 surface maps, and appear to follow the same spatial characteristics as more central RFs (see supplemental Fig. S2, available at www.jneurosci.org as supplemental material).

Results

The mapping of the visual field onto primary visual cortex

Although it has become common to use flat map visualizations of cortex, measurement of distances on the cortical surface are inherently distorted by flattening procedures (Engel et al., 1997; Fischl et al., 1999; Van Essen et al., 2001; Polimeni et al., 2006), thus a nonflattened model was used here for both measurement and visualization. The model of V1 proposed by Daniel and Whitteridge (1961) was the first clear quantitative description of the transformation of visual spherical space onto a surface sheet representing V1 using the cortical magnification factor (CMF). Recognizing that the appropriate visual reference frame was a spherical coordinate system centered at the eye, they visualized the mapping problem by scaling an isoeccentric ring by the magnification factor for a discrete position in eccentricity. The V1 surface was then constructed by generating a series of such rings as a function of eccentricity. The incremental spacing of each ring was derived from the ring radius and the length increment calculated for an advance along a meridian. Constructed in this manner the projection of the visual field defines a curved three-dimensional surface. Unfortunately, the V1 surface illustrated in Figures 5 and 6 of their study (p. 213), and widely cited, differs slightly but significantly from the mathematical description posed by Daniel and Whitteridge (1961). The V1 surface depicted in their figures shows the expansion of the foveal area and a continued radial expansion of the V1 surface up to ~20° eccentricity and then a continuous decrease in the radial dimension of the surface ending with a meeting of the vertical and horizontal meridians forming a closure of the surface in the extreme peripheral eccentricity. However, such a closure and meeting of the meridians is not possible using the logic and equations provided in their study. The equations and CMF used by Daniel and Whitteridge (1961) contain an explicit assumption of isotropy that precludes an actual closure of the V1 surface in the far periphery. The surface cannot actually close and the meridians cannot meet unless the isotropy constraint is dropped and the inverse cortical magnification factor becomes infinite.

The surface realization method of approximations used by Daniel and Whitteridge (1961) is equivalent to the derivative based surface mapping equations provided by Rovamo and Virsu (1984). This set of equations map visual space to a surface using the CMF, assuming only a single constraint, local isotropy, for the mapping process. Using a spherical coordinate system these equations specify the exact mapping of visual space to a curved surface. Both space and the curved surface are azimuthally symmetric, therefore a plot of a meridian (increasing eccentricity from fovea) describes the profile of the surface. The equations define the position along a meridional slice through the surface with the surface generated by rotating the slice through the azimuthal range. Each point in visual space $\mathbf{v}(\theta,w)$ is described by azimuth θ and eccentricity w and associated with a corresponding point in cortical space $\mathbf{c}(r,z,\phi)$ described by the radius r of the 3D model surface at that eccentricity (Fig. 1), the distance z along the axis of rotation (both given in millimeters), and a rotational angle ϕ (identical to the azimuthal angle θ), according to the following set of equations by Rovamo and Virsu (1984):

$$r = M(w)\sin w$$

$$z = \int_0^w [M(w)^2 - (dr/dw)^2]^{0.5} dw$$

$$\phi = \theta.$$

The surface profile is unique for each cortical magnification factor (M; in millimeters per degree). The CMF is also uniquely

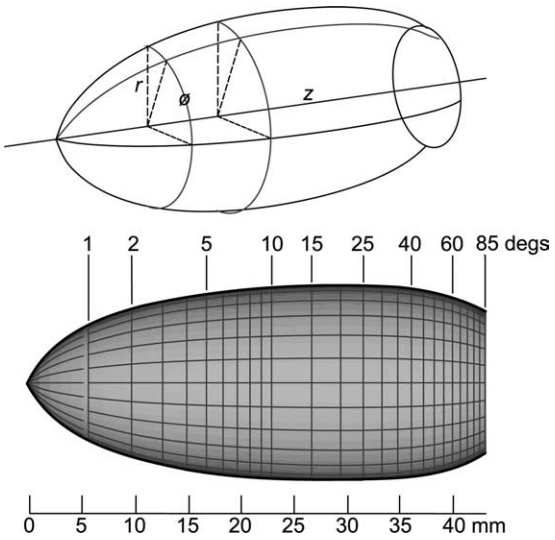

Figure 1. 3D model of the surface of striate visual cortex. Top, The location of an object in visual space is defined by its eccentricity (w) along a meridian angle (θ). This spherical coordinate position maps to a location (r,z,ϕ) on a smoothly curved three-dimensional surface. The equations for the mapping (Rovamo and Virsu, 1984) use the cortical magnification factor and the assumption of local isotropy. For the macaque magnification factor used here, the result is an elongated curved surface extending ~43 mm from foveal tip to far periphery. Bottom, Viewed from the side the meridian lines meet in the fovea to the left. The meridian lines do not meet at a point in far periphery but end along an arc as shown on the right. In the figure the meridian lines representing increments of 15° are crossed by vertically aligned lines of equal eccentricity incrementing in degrees as indicated by the drop lines above.

defined for each individual as the mapping between the area of the visual field laid out in spherical coordinates and the area of that individual's V1 surface. There is no empirical evidence that the function describing the general form of the CMF changes within the order of primates. Changes in the parameters are sufficient to accommodate the variations in areal size of V1 among members of a species as well as between species within a genus. The CMF used here for macaque monkeys is taken from LeVay et al. (1985) as an average estimate appropriate to the brain sizes estimated for the animals used in this study, expressed there in terms of areal magnification as $M_a = 100(0.8 + w)^{-2.0}$, where w is eccentricity in degrees and magnification is square millimeters of cortex per square degree of visual field. Although various local anisotropies may occur in isoeccentric or meridian axes, the product in local areas is often relatively constant in terms of areal magnification (Van Essen et al., 1984; LeVay et al., 1985; Tootell et al., 1988; Adams and Horton, 2003; Schiessl and McLoughlin, 2003). Given that anisotropy has been reported as an average azimuthal compression, rather than as separate local values from which an adjusted model could be made, and given that reported anisotropies have been rather specific to individuals, the decision here was to forego any attempt to impose any correction of the simple single CMF based surface. Using the areal magnification values the area of the generated surface on the model matches closely the reported total area of V1 in those studies that report both factors (Van Essen et al., 1984; Gattass et al., 1987; Fritsches and Rosa, 1996).

Using the above equations a 3D reconstruction of the surface of macaque monkey primary visual cortex was made (Fig. 1). In Figure 1 the fovea is at the tip of the model on the left and the far periphery at 85° eccentricity is shown as the circle at the far right. Lines that run from fovea to periphery are meridians of the spherical coordinate system, and circles perpendicular to the z-axis are equal eccentricity bands with ϕ equivalent to the theta angle of the spherical coordinate system. Using the above CMF estimate, the V1 surface area of the model represents 1110 sq mm per hemisphere with a z-axis of ~43 mm.

V4 receptive fields are elongated along meridians of the visual field

The activity of neurons with RFs in the lower contralateral quadrant of the visual field was recorded in four rhesus monkeys. Postmortem examination of the electrode placements within a grid marked by reference pins indicated that all recordings came from the mid to caudal portion of the crown of the prelunate gyrus at or below the level of the tip of the lateral sulcus. This area receives projections from V2 and is consistent with that portion of dorsal V4 termed the caudal dorsolateral visual complex (Shipp and Zeki, 1985; Nakamura et al., 1993; Stepniewska et al., 2005). RF maps and stimulus preference characterizations were completed in 337 neurons that serve as the database for this study. RFs were mapped using a flashed stimulus presented in a random sequence of positions defined by a 16 by 16 grid during each fixation trial. An adaptation of the reverse correlation method was used to calculate response activity as a function of stimulus position. RFs were then depicted as activity gradients in contour plots.

The RFs of the vast majority of V4 neurons responding to flashed stimulus presentations are elongated along the meridians radiating outward from the fovea as shown on the left in Figure 2. The contours mark 12.5% increments of responsiveness from baseline to the peak activity in the central "hot spot." The elongation causes the response amplitude contours to appear as distorted concentric circles stretched along all meridians. The stretching of the RFs is also apparent in terms of the steepness of the response gradients within the receptive fields. With respect to the central hot spot the activity contours are compressed toward the fovea and expanded toward the periphery. Most (>90%) V4 cells tested were sensitive to stimulus orientation using an orthogonal min/max response rate index of <0.8 to define orientation sensitivity. The preferred stimulus orientation sensitivity of these V4 neurons had only a weak correlation with the angle of the meridian passing through the receptive field (see supplemental Fig. S1, available at www.jneurosci.org as supplemental material).

The asymmetry of the response profile with respect to peak discharge location was confirmed under more standard stimulus presentation conditions by presenting stimuli at eight locations along a radial line that passed from the fovea through the center of the hot spot. Stimuli were flashed (200 ms on, 400 ms off) at each location using a random permutation sequence and 3–7 flash cycles per trial while the animal fixated. Figure 2 compares the two techniques, depicting the contour plot derived from the grid presentation with raster displays of the activity evoked at 8 locations along a radial slice through the RF (Fig. 2*B*). The slice through the RF profile produced by the standard presentation method matches the profile obtained with the reverse correlation method and confirms the use of the technique for measurement of RFs. A small minority of neurons had broad central peak areas or, alternatively, lacked any clear organization within the RF border. These neurons resulted in poorer RF fits as discussed below; resulting in 15 of 337 neurons having fitting errors >2 SDs from the mean error score. Subfield organization was not evident using a single stimulus that was optimal within the set tested. Response profiles peaked at one location within the RF, typically biased toward the fovea, and gradually subsided toward the RF border.

The consistent biased positioning of the hot spot within the RF argues that the stimuli were revealing a common spatial structure for V4 RFs. Others have reported subfield organizations within V4 RFs, for example, when comparing responses to stimuli of different contrast, when using multiple stimuli or when using analyses based on extended surfaces (Desimone and Schein, 1987; Pollen et al., 2002; Clarke and Paradiso, 2004). It is possible that each subfield shares the overall mapping principle, but the data presented here cannot argue for or against that hypothesis.

In Figure 2, a small bar was optimal for the neuron. That stimulus is shown in the upper left, scaled and oriented as it was used to produce the RF contour plot shown below it. The majority of V4 neurons (62%; 173/279) studied in a quantitative size series preferred stimulus sizes smaller than the RF width. A significant minority of V4 neurons (30%; 85/279) increased their responses to increasing stimulus size up to the width of the RF and then reduced responsiveness to further increases in stimulus size, a result consistent with a suppressive surround (Desimone and Schein, 1987). In this study optimally large stimuli were reduced in size to a smaller faction of the RF size for mapping purposes.

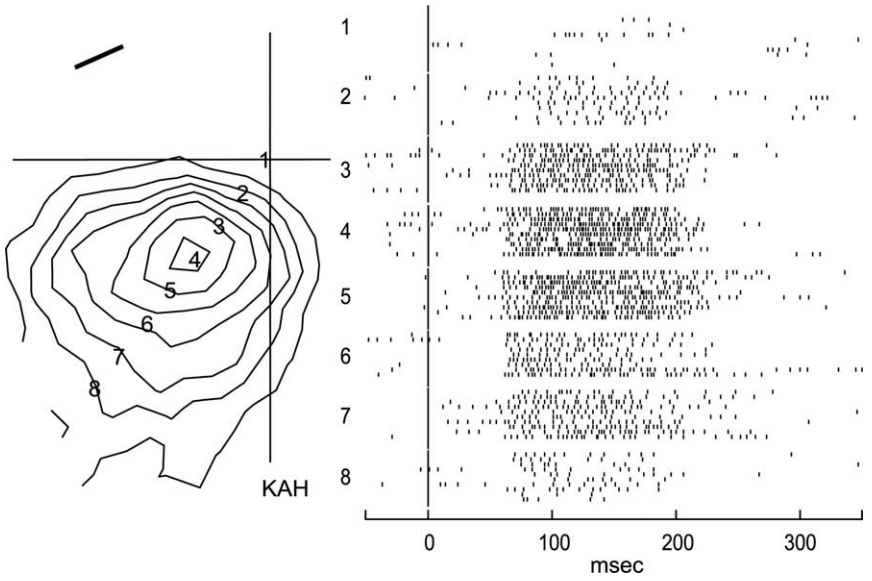

Figure 2. Response amplitude contour plot of V4 receptive field. The receptive field is distorted from circular symmetry with respect to the hot spot by compression toward the fovea (center of the horizontal and vertical axis) and expansion toward the periphery. The receptive field contours are based on responses to a short bar (illustrated to scale in the upper left) delivered in rapid succession on a 16 × 16 grid. Responses in raster format to a separate series of flashed stimuli delivered at eight locations (marked with numerals) from fovea to periphery and cutting through the receptive field are shown on the right. Small vertical tics in each row of the raster represent the time of neuronal discharge; each row represents a single presentation of the stimulus at time 0, grouped according to the eight different stimulus locations. Eccentricity of receptive field center is 2.5°.

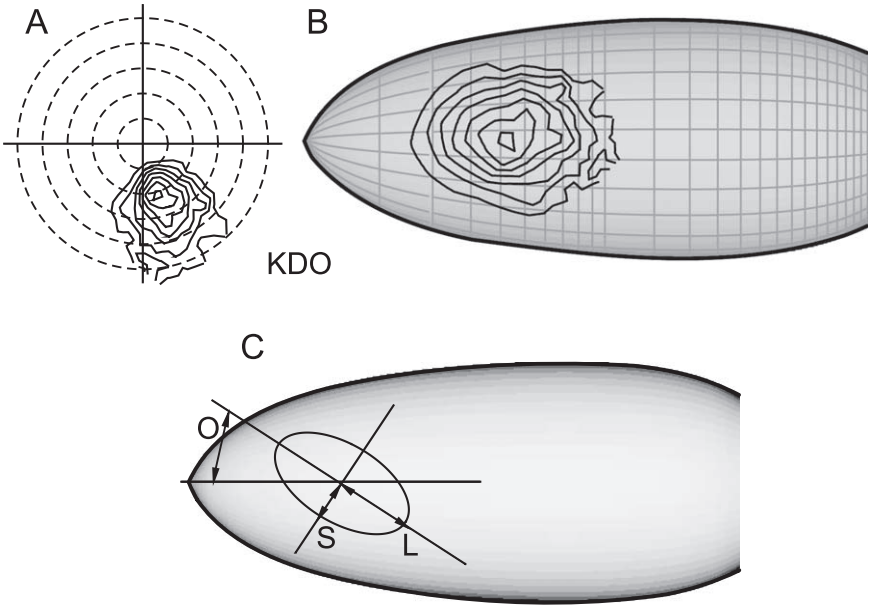

Figure 3. Back projection of V4 receptive field onto the V1 model surface. ***A***, Distorted receptive field as it appears in normal space mapping. Eccentricity dashed lines at 2° intervals. ***B***, Same receptive field replotted on surface of the V1 model. The apparent circularly symmetric contour plot lines indicate the distortion is the result of the visual field representation at the level of the V1 map. Note the V1 surface is a curved 3D surface seen here as an orthographic projection. ***C***, To measure the symmetry of the receptive field map on V1 surface the receptive field was fitted to a bivariate Gaussian surface. A ratio of the short (S) to long (L) axes of the fit served as an index of the circularity of the receptive field. This index was computed for various orientations (O) of the long axis of the Gaussian with respect to the meridian projecting from fovea to periphery through the RF center.

The elongation of the V4 receptive fields is produced by the V1 CMF

The elongated contour profile suggests an underlying magnification process with a differential stretch of the RF along an axis of eccentricity. The working hypothesis was that the elongation reflects the V1 CMF. Under this hypothesis V4 RFs represent a Gaussian sampling obtained from neurons across the topography of the V1 surface that is itself distorted in its representation of visual space by the CMF. If the elongated distortion of V4 RFs reflects a simple sampling of a distorted V1 topography, then a projection of the V4 contours onto the V1 topography should remove the distortion. The back projection technique is the equivalent of a mathematical transform that removes the V1 CMF. This back projection of V4 contours onto the V1 surface simply changes the mapping from the coordinate system of external visual space to the coordinate system of V1. To visualize this relationship the V4 RF contours were projected onto a 3D model of the V1 surface. As can be seen in Figure 3, the projection of a distorted V4 RF contour appears as a set of concentric circles on the curved surface of the V1 model. This is exactly what would be expected from a simple convergence of information from V1 to V4. If there had been an additional eccentricity-dependent gain between V1 and V4, then one would expect some residual eccentricity dependent stretching along the meridians from fovea to periphery. The projections appear to be simple circles, indicating that the deformation is completely attributable to the V1 magnification factor. To quantify the "circle" appearance of the RF projection, each RF projection onto the V1

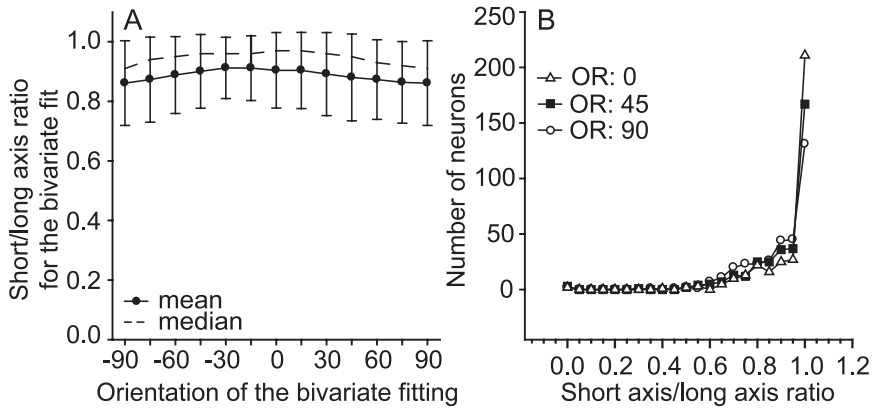

Figure 4. Circular symmetry of the back-projected receptive fields. ***A***, Median and mean (±1.0 SD) values of the short/long axis ratio for the bivariate fits as a function of the orientation of the long axis of the Gaussian with respect to the meridian that passed through the receptive field center. Additional eccentricity dependent cortical magnification after V1 should produce a minimum near 0, where the long axis parallels the meridian and the short axis is iso-eccentric. There is no evidence for this case. ***B***, The distribution of ratio values at three different analysis orientations for the population of 337 neurons. A large majority of the neurons (238/337) have a ratio index >0.90 for the orientation (OR:0) that parallels the meridians indicating a circular symmetry. OR, Orientation of the long axis of the Gaussian fit with respect to the meridian.

surface was fit by a bivariate Gaussian contour. The ratio of the short to long axis of the best fit was used as an index of the circularity of the RF. The locations of the 16 × 16 array of data and the estimated hot spot were converted into location coordinates on the V1 surface. The millimeter distances between the points on the surface were then measured by integrating the distance traversed as one moves between the points in integrals steps while maintaining the correct $dz/d\phi$ ratio where z is the long axis of the surface and ϕ is the visual field angle between the points. A minimum least squares bivariate Gaussian fit was performed on the 16 × 16 array as transformed into the millimeter scaling.

The hypothesis is that there is no systematic distortion along a meridian of the visual field; such a distortion would reflect an eccentricity dependent magnification. However, distortions away from perfect circularity can be expected by elongations in the RF map resulting from actual idiosyncratic RF shapes or chance distortions of the RF during the RF mapping. Therefore the ratio was calculated as a function of the orientation of the long axis of the Gaussian fit with respect to a meridian (Fig. 3*C*) to assess any systematic bias. Note that throughout this section the term "orientation " refers to the orientation of the Gaussian fit not to a neuron's sensitivity to stimulus orientation. Any eccentricity dependent magnification should produce smaller ratios when the long axis of the fitting analysis aligns with the meridian passing through the RF center compared with other orientations of the fitting analysis. The fitting process was repeated in 15° steps of orientation of the long axis away from a meridian. A short/long axis ratio of 1.0 indicates a circular fit and a lack of elongation with respect to the orientation of the Gaussian fit. For each orientation of the bivariate Gaussian the median (dashed) and average (solid) axis ratio was determined across the population of 337 neurons, the results are shown in Figure 4*A*. The average short/long axis ratio is 0.89 (median 0.95) across the 12 different fitting orientations examined. The average SD within each orientation measure was 0.13. If there were further eccentricity dependent gain changes, then the result should be a decrease in the ratio for the orientation that parallels the meridians. The results suggest a slight tendency, if anything, for an increase in the ratio for that orientation of the analysis, the 0 orientation in Figure 4*A*. These results therefore essentially rule out any further eccentricity dependent magnification between V1 and V4. The average short/long axis ratio that parallels the meridian through each RF center is 0.90 (median 0.97). The ratio distributions are heavily skewed to a value of 1.0 as shown by plotting the ratios for the 337 neurons in Figure 4*B* at each of three different analysis orientations. A substantial majority of the neurons (211/337 for the axis that parallels the meridian) were best fit by a short/long axis ratio of 1.0 at each orientation of the bivariate Gaussian, indicating that the V1 cortical magnification factor does in fact account for the distortion of the V4 RFs. The distributions of the ratios indicate the projection of the V4 RFs onto V1 can be reasonably characterized as univariate or circular representations. The fact that the distributions profiles were the same across analysis orientations indicates there was no evidence for an eccentricity dependent magnification beyond area V1.

The size of V4 receptive fields represents a constant sampling area of V1

Figure 5 illustrates the back projection of three V4 RFs onto the surface of V1. The three RFs have very different sizes as seen in the visual space plots of the receptive fields on the left but are associated with nearly equivalent areas on the surface of V1. The hypothesis drawn from this observation is that the forward projection that produces V4 RFs represents a convergence onto V4 neurons of visual field information arising from comparable areas (in square millimeters) of V1 regardless of eccentricity (see also supplemental Figure S2, available at www.jneurosci.org as supplemental material). To examine this issue the SD of the minimum least squares univariate Gaussian fit (SDfit) of the V4 RFs onto the V1 surface was determined using the 16 × 16 mapping data set. The SDfit measure is in millimeters of cortex along the curved V1 surface model. The average SDfit for the population is 3.8 mm with a range of ~2–6 mm. It is important to note that the estimates for the SDfit are tied directly to the cortical magnification factor used to create the V1 surface model. It is not known whether the sampling area changes with changes in the total areal size of V1.

Figure 6*A* shows that the SDfit measure does not change as a function of the eccentricity of the receptive field center over the central 10° that the data covers. This observation supports the hypothesis that V4 neurons sample the V1 topography using the same scale of convergence independent of eccentricity, thereby implying that the scale of the spread of the anatomical connections from V1 to V4 is the same from fovea to periphery. The vastly different V4 RF sizes (Fig. 5) simply reflect the scale of the V1 topography from which the V4 neuron receives information. Based on the illustrations in Figures 3 and 5 it is clear that each V4 neuron receives information from a large part of the V1 surface. For example, the neuron in Figure 3 has a SDfit value of 3.6 which is nearly the average for the population. If twice the average SD is used as an estimate of the total radius of sampling on V1 then the sampling area is ~180 mm^2 which represents ~1/6 of the total V1 hemispheric surface area; a value that emphasizes the remarkable degree of convergence from V1 to V4.

The scatter of the SDfit data at each eccentricity in V1 (Fig.

6*A*) reflects the local scatter of RF size in area V4, plus any error resulting from either an imperfect modeling of the RF projection by a univariate Gaussian model or factors related to the mismatch between the assumed cortical magnification factor (CMF) and the actual CMFs for each monkey. Certainly each receptive field was not a perfect match to a model RF. However, if some of the scatter were caused by CMF mismatches then one would expect that the correlation between measures would be affected by both an eccentricity variable that would reflect differences between the model CMF and the actual CMF and a subject variable that would account for CMF differences between monkeys. A multilinear regression was therefore performed to consider RF size, eccentricity (RFecc) and monkey subject. The V4 RF areas were measured at one half the maximum response amplitude above the background activity level. The measure of RF size is reported as the square root of the RF area lying within the half amplitude RF contour. All three variables contributed ($p < 0.01$) to predicting the SDfit, where SDfit = 3.58 + 0.60 RF size − 0.51 RFecc − 0.11 subject ($r = 0.90$). The presence of effects in all three variables is consistent with differences in the CMF generating some of the scatter in the RF fitting process, although without the actual CMFs it is not possible to sort out the other factors. The variability of the fits is therefore probably overestimated.

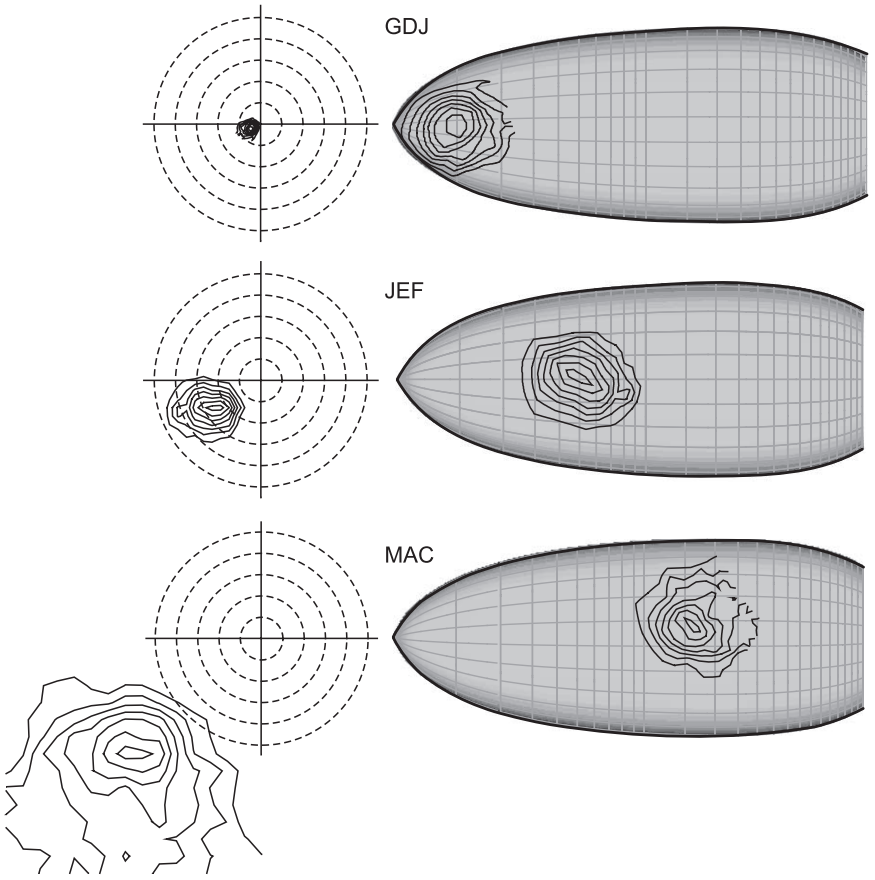

Figure 5. Equal-sized back projections. Left, The two-dimensional visual space illustration of the contour response amplitude receptive fields of three V4 neurons centered, respectively, at eccentricities of 1.0, 5.0, and 15.8°. The dashed circles represent lines of eccentricity at 2, 4, 6, 8, and 10°. Right, Back projections onto the V1 surface for the three V4 neurons. The very different-sized V4 receptive fields map to essentially the same size on the V1 surface, indicating that receptive fields in V4 are constructed from information converging from equivalent circular anatomical patches in V1.

Receptive field size as a function of eccentricity in V4

Figure 6*B* depicts the V4 RF size (gray circles) as a function of the eccentricity of the RFs hot spot, visually estimated at the center of the innermost response contour. The dashed line depicts a least squares linear regression of RF size on eccentricity (RFecc) that yielded: RF size = 1.39 + 0.71 RFecc ($r = 0.58$). As a rough estimate it appears that the diameter of V4 RFs at their half maximum response amplitude is approximately equal to their eccentricity. The data presented in Figure 6*B* indicate larger V4 RFs than previously reported when based on hand mapping techniques (Tanaka et al., 1986; Desimone and Schein, 1987; Gattass et al., 1988). Although the regression slopes are generally similar, the RF size in this study is based on the half amplitude response measure and thus overall RF size is much larger. Using the RF modeling in the feed forward direction, the size of V4 RFs can be further appreciated by considering that a normal curve with a SD of 3.8 mm falls to about half amplitude at 4.5 mm. The area of the visual field (a model half amplitude RF) enclosed by a circle of radius 4.5 mm drawn on the curved surface of the V1 model was calculated for various eccentricities. The solid diagonal line in Figure 6*B* represents the square root of those area measures and provides confirmation of the relationship between

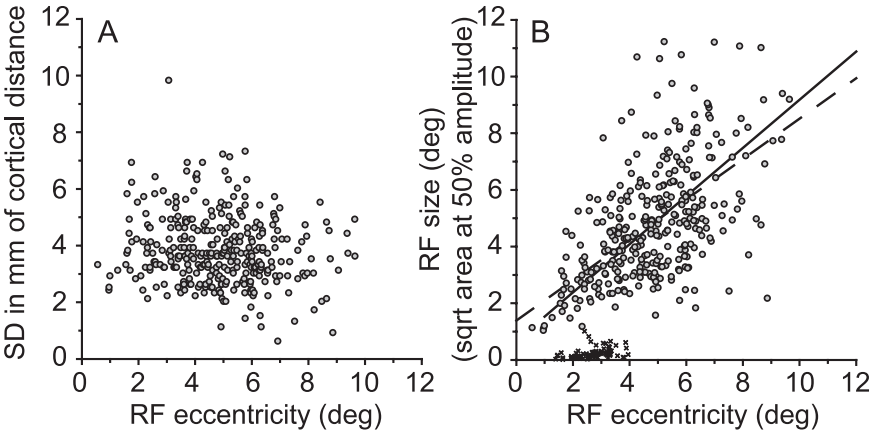

Figure 6. V1 sampling size and receptive field size. The SD of a univariate Gaussian fit (SDfit) of the V4 back projected receptive fields (RF) are used to estimate the size of the sampling area in primary visual cortex ($n = 337$). ***A***, The size of the sampling areas does not change as a function of eccentricity with a mean SDfit of 3.8 mm. ***B***, V4 RF size as a function of RF eccentricity (gray circles) where RF size is the square root of the area contained by a contour at half the maximum response amplitude. Dashed line is the linear regression of the V4 data. Solid line is the prediction of the RF size based on the sampling of the V1 cortical surface using a radius of 4.5 mm which represents the half amplitude of a two-dimensional Gaussian for the fitted data. Crosses in lower left represent similarly measured RF sizes in area V1 ($n = 83$).

V4 RF size and a circular sampling of the V1 surface by closely approximating the dashed line of the linear regression of measured RF size as a function of eccentricity.

The mapping technique was also applied to neurons recorded in area V1 to obtain a direct comparison reference for the different RF sizes in the two cortical areas. RF maps were obtained from V1 neurons directly across the prelunate sulcus from the V4 recording sites in one animal ($n = 83$). RF maps from V1 neurons were obtained using very small rectangular bars, lines or dots. Eye position fixation requirements during V1 recording were reduced to a 0.3° radius constraint. The V1 RF sizes (square root of area) are plotted as small crosses along the bottom of Figure 6*B* between 2 and 4° of eccentricity. The dramatic change in RF size underscores the massive convergence that takes place in the visual system in only two primary steps, V1 to V2 to V4, and complements the picture of the back projected V4 RFs on the surface of V1 in Figures 3 and 5.

Discussion

Receptive fields of neurons in the posterior crown of the prelunate gyrus of dorsal area V4 represent the lower visual field. This study has shown that the V4 receptive fields (RF) have an asymmetry in both RF shape and position of peak sensitivity within the RF. This asymmetry is completely determined by the transformation of visual space according to the cortical magnification factor for primary visual cortex, area V1. The analysis provided in this report demonstrates that a V4 receptive field represents a convergence of information drawn from a circular patch of V1. The response sensitivity profile of a V4 neuron's RF matches a circularly symmetric Gaussian sample of V1 that can be graphically illustrated by back projecting the response sensitivity contour map of a V4 RF onto a surface model of area V1. Quantitative measures of the aspect ratio of the back projected contour are near 1:1, indicating that there is no further eccentricity dependent magnification of the visual field between areas V1 and V4. This result emphasizes the importance of area V1 in establishing the spatial framework for cortical visual processing.

The RF profile of V4 neurons as measured in this experimental series consistently revealed a simple Gaussian profile. Previous reports of subfield components in V4 typically involved the use of multiple simple stimuli opposed in luminance or color (Desimone and Schein, 1987; Pollen et al., 2002; Freiwald et al., 2004). The emphasis of the present study was to use the best single stimulus chosen from a set of slightly more complex shapes that often produce quite robust responses from V4 neurons. A single "optimal" stimulus was a practical choice to map the broad extent of the RFs of V4 neurons. Using such a stimulus, it is perhaps expected that the representation is Gaussian in form. The issue pursued in this study is the extent to which spatial representation is determined by the topography of the areas that give rise to input to V4 neurons. The scale of the V1 sampling area by V4 neurons also minimizes issues concerned with the fine grain of the visual field representation. Although there are discontinuities the V1 visual field representation within layer 4 related to the monocular ocular dominance columns (Blasdel and Fitzpatrick, 1984), in the binocular driven superficial layers that give rise to the feed forward projections those discontinuities are not apparent but, if present, are most likely inconsequential at the scale of convergence of the projections to V4.

The back projected V4 receptive fields as they appear on the V1 surface model all result in circular patches whose size is independent of eccentricity. The constant sized, circular back-projected patches also represent regularity in the convergence of information from one visual cortical area to another. This is a relatively simple and elegant pattern of connection that has previously been suggested by anatomical studies but not functionally demonstrated (Rockland and Virga, 1990; Rockland, 1992). The bulk of the anatomical projection from V1 to V4 passes through V2 (Felleman and Van Essen, 1991). The size of the circular back projected patches relative to the total size of the V1 area indicates a remarkable systematic convergence established after the relay through area V2. This precision is especially notable because the anatomical projection fields from V2 to V4 originate from the interstripe and thin stripe zones of the segregated visual field representations in area V2 (Shipp and Zeki, 1985; Nakamura et al., 1993; Roe and Ts'o, 1995). In fact, the projection to V4 from the segmented V2 visual field representations indicates that the circular sampling patches are not a general model for all cortical-cortical connection schemes, at least at a small scale of connectivity. The V4 neurons do not appear to inherit any of the distortions present in the topography of the retinotopic mapping in V2. The projections from V2 to V4 and the consequent sampling of those projections by V4 neurons must compensate for both the discontinuities in the V2 visual field representation and the field anisotropies noted within V2 stripes (Roe and Ts'o, 1995; Shipp and Zeki, 2002). The current study emphasizes that the spatial scale of the RFs of V4 neurons faithfully reflects a linear V1 magnification without the anisotropies of intermediate areas. The conclusion is that the existence of cortical visual field anisotropies in antecedent areas do not mandate similar receptive field anisotropies in the target projection areas. Furthermore the existence of topographic visual field anisotropy (including cortical magnification) in the map of a cortical area does not necessarily imply receptive field anisotropy in that area, and conversely, the lack of receptive field anisotropy does not imply a lack of topographic visual field anisotropy. These observations are consistent with a suggestion that expanded or anisotropic representations of the visual field in extrastriate areas may reflect the existence of multiple interdigitated modular zones within a cortical area rather than a new magnification of spatial interactions. This form of cortical expansion could allow modules handling different featural processing within a cortical area to maintain a constant spatial magnification factor within RFs across cortical areas. The spatial relationships of objects with receptive fields are therefore not necessarily distorted by changes in the overall cortical magnification of the cortical area. Ultimately perhaps this suggests that the differential expansion of peripheral versus central processing in dorsal versus ventral visual systems is an emphasis on processing modules rather than actual anisotropies in the representation of space. Of course this does not rule out RF anisotropies. The existence of extremely elongated receptive fields reported in anterior V4a in primates (Pigarev et al., 2002) and in areas 7, 21a and claustrum of cats (Sherk and LeVay, 1981; Rodionova et al., 2004) may specifically represent special RF adaptations for the processing of particular types of visual information, particularly visual motion. The elongated RFs may likewise be independent of the visuotopic map of those areas.

The orthographic projection of the V1 surface as drawn by Daniel and Whitteridge (1961) has been at odds with anatomical studies of the peripheral edge of V1, particularly as shown by the 2-deoxy-D-glucose (2-DG) studies of ocular dominance columns in V1 (LeVay et al., 1985). According to the 2-DG studies the peripheral edge of V1 ends in an extended monocular edge rather than as a narrow monocular region squeezed between the upper and lower binocular field representations of the vertical meridian as predicted by the Daniel and Whitteridge (1961) representa-

tion. This discrepancy is resolved by the plots of the visual field shown in Figure 1, where the meridians are shown not to meet but rather end on an arc that is the extended edge of the peripheral visual field. This result is actually inherent in the equations and methods presented in their original 1961 study but were not followed in the construction of their two-dimensional orthographic projection figure.

The constant size of the back projected V4 RF patches and their position on the V1 surface model pose an interesting question as to what happens when the patch representation approaches either end of the surface. At the foveal end a circular patch centered on the fovea covers approximately the central degree of the visual field extending into both contralateral and ipsilateral space. This observation is consistent with anatomical and RF plots that depict the foveal representation of the V4 vertical meridian in both hemispheres with overlap into ipsilateral space (Van Essen and Zeki, 1978). On the other hand, as the circular patches move outward in eccentricity along the model surface it becomes clear that a circular patch, centered at ~40° eccentricity, samples space out to the edge of the peripheral visual field. If the center of the RF representation were to extend beyond ~40° in eccentricity, then the circular sampling profile must be truncated and the central peak of activation might be displaced toward the far edge of the RF. An alternative hypothesis is that there is no reason to extend the center of the sampling beyond 40° as the remainder of the peripheral visual field is represented within the RFs centered at 40°. Relatively little is known about the processing of information at these far eccentricities. Electrophysiological studies have reported that various visual areas actually lack representations of the peripheral visual fields. In particular dorsal V4 has been found to lack peripheral RFs centered beyond ~40–50° (Gattass et al., 1988; Boussaoud et al., 1991). Imaging techniques can have a similar spatial registry problem when they base a peripheral location estimate on the center of an activated region that corresponds in temporal registry with the stimulus position. The large RFs of peripheral areas make it difficult to be precise with regard to stimulus position and eccentricity. In fact the expansion in the size of the RFs at successive levels of the visual hierarchy may actually contribute to the apparent contraction of the overall topographic representation of visual space in a cortical area.

Finally, the constant size of the V4 back-projected RFs suggests a possible substrate for the mechanism of the critical spacing requirement between target and nearest distractor observed for detection performance in visual search. The critical spacing (~7 mm for monkey) has been shown to be independent of eccentricity and spatially scaled to distances along the surface of V1 by the cortical magnification factor (Motter and Holsapple, 2000; Motter and Simoni, 2007). An analogy can be drawn between the visual crowding of detection performance and interference between a target at the center of a RF and the interference resulting from a distracter that enters the RF (Moran and Desimone, 1985; Motter, 2002). The size of V4 receptive fields match well with a general rule of visual crowding that states that visual crowding occurs when the separation between target and distractor are within one half the target eccentricity (Bouma, 1970; Motter and Simoni, 2007). These comparisons suggest that integration within V4 receptive fields may play an important role in visual crowding phenomena. The understanding of perceptual phenomena based on cortical magnification scaling however is not overly constrained by these findings, as the basis for perceptual phenomena is most likely weighted by the number of neurons involved as well as by what occurs within their receptive fields. Cortical topographic maps of function provide a basis for estimating the relative numbers of neurons.

References

Adams DL, Horton JC (2003) A precise retinotopic map of primate striate cortex generated from the representation of angioscotomas. J Neurosci 23:3771–3789.

Blasdel GG, Fitzpatrick D (1984) Physiological organization of layer 4 in macaque striate cortex. J Neurosci 4:880–895.

Bouma H (1970) Interaction effects in parafoveal letter recognition. Nature 226:177–178.

Boussaoud D, Desimone R, Ungerleider LG (1991) Visual topography of area TEO in the macaque. J Comp Neurol 306:554–575.

Clarke C, Paradiso M (2004) The complex spatial topography of attentional modulation in macaque V4. J Vision 4:7a. Retrieved April 20, 2009 from http://journalofvision.org/4/8/7/.

Daniel PM, Whitteridge D (1961) The representation of the visual field on the cerebral cortex in monkeys. J Physiol 159:203–221.

Desimone R, Schein SJ (1987) Visual properties of neurons in area V4 of the macaque: sensitivity to stimulus form. J Neurophysiol 57:835–868.

Engel SA, Glover GH, Wandell BA (1997) Retinotopic organization in human visual cortex and the spatial precision of functional MRI. Cereb Cortex 7:181–192.

Felleman DJ, Van Essen DC (1991) Distributed hierarchical processing in the primate cerebral cortex. Cereb Cortex 1:1–47.

Fischl B, Sereno MI, Dale AM (1999) Cortical surface-based analysis II: inflation, flattening, and a surface-based coordinate system. Neuroimage 9:195–207.

Freiwald WA, Tsao DY, Tootell RBH, Livingstone MS (2004) Complex and dynamic receptive field structure in macaque cortical area V4d. J Vision 4:184a. Retrieved April 20, 2009 from http://journalofvision.org/4/8/184.

Fritsches KA, Rosa MGP (1996) Visuotopic organisation of striate cortex in the marmoset monkey (*Callithrix jacchus*). J Comp Neurol 372:264–282.

Gattass R, Sousa AP, Rosa MG (1987) Visual topography of V1 in the *Cebus* monkey. J Comp Neurol 259:529–548.

Gattass R, Sousa AP, Gross CG (1988) Visuotopic organization and extent of V3 and V4 of the macaque. J Neurosci 8:1831–1845.

Gattass R, Nascimento-Silva S, Soares JG, Lima B, Jansen AK, Diogo AC, Farias MF, Marcondes M, Botelho EP, Mariani OS, Azzi J, Fiorani M (2005) Cortical visual areas in monkeys: location, topography, connections, columns, plasticity and cortical dynamics. Philos Trans R Soc Lond B Biol Sci 360:709–731.

LeVay S, Connolly M, Houde J, Van Essen DC (1985) The complete pattern of ocular dominance stripes in the striate cortex and visual field of the macaque monkey. J Neurosci 5:486–501.

Moran J, Desimone R (1985) Selective attention gates visual processing in the extrastriate cortex. Science 229:782–784.

Motter BC (1994) Neural correlates of attentive selection for color or luminance in extrastriate area V4. J Neurosci 14:2178–2189.

Motter BC (2002) Crowding and object integration within the receptive field of V4 neurons. J Vision 2:274a. Retrieved April 20, 2009 from http://journalofvision.org/2/7/274.

Motter BC (2006) Modulation of transient and sustained response components of V4 neurons by temporal crowding in flashed stimulus sequences. J Neurosci 26:9683–9694.

Motter BC, Holsapple JW (2000) Cortical image density determines the probability of target discovery during active search. Vision Res 40:1311–1322.

Motter BC, Holsapple JW (2001) Separating attention from chance in active visual search. In: Visual attention and cortical circuits (Braun J, Koch C, Davis JL, eds), pp 159–175. Cambridge, MA: MIT.

Motter BC, Simoni DA (2007) The roles of cortical image separation and size in active visual search performance. J Vision 7:6.1–15. Retrieved April 20, 2009 from http://journalofvision.org/7/2/6.

Motter BC, Simoni DA (2008) Changes in the functional visual field during search with and without eye movements. Vision Res 48:2382–2393.

Nakamura H, Gattass R, Desimone R, Ungerleider LG (1993) The modular organization of projections from areas V1 and V2 to areas V4 and TEO in macaques. J Neurosci 13:3681–3691.

Pigarev I, Nothdurft H, Kastner S (2002) Neurons with radial receptive fields in monkey area V4A: evidence of a subdivision of prelunate gyrus based on neuronal response properties. Exp Brain Res 145:199–206.

Polimeni JR, Balasubramanian M, Schwartz EL (2006) Multi-area visuotopic map complexes in macaque striate and extra-striate cortex. Vision Res 46:3336–3359.

Pollen DA, Przybyszewski AW, Rubin MA, Foote W (2002) Spatial receptive field organization of macaque V4 neurons. Cereb Cortex 12:601–616.

Rockland KS (1992) Configuration, in serial reconstruction, of individual axons projecting from area V2 to V4 in the macaque monkey. Cereb Cortex 2:353–374.

Rockland KS, Virga A (1990) Organization of individual cortical axons projecting from area V1 (area 17) to V2 (area 18) in the macaque monkey. Vis Neurosci 4:11–28.

Rodionova EI, Revishchin AV, Pigarev IN (2004) Distant cortical locations of the upper and lower quadrants of the visual field represented by neurons with elongated and radially oriented receptive fields. Exp Brain Res 158:373–377.

Roe AW, Ts'o DY (1995) Visual topography in primate V2: multiple representation across functional stripes. J Neurosci 15:3689–3715.

Rovamo J, Virsu V (1984) Isotropy of cortical magnification and topography of striate cortex. Vision Res 24:283–286.

Schiessl I, McLoughlin N (2003) Optical imaging of the retinotopic organization of V1 in the common marmoset. Neuroimage 20:1857–1864.

Sherk H, LeVay S (1981) The visual claustrum of the cat. III. Receptive field properties. J Neurosci 9:993–1002.

Shipp S, Zeki S (1985) Segregation of pathways leading from area V2 to areas V4 and V5 of macaque monkey visual cortex. Nature 315:322–325.

Shipp S, Zeki S (2002) The functional organization of area V2, II: The impact of stripes on visual topography. Vis Neurosci 19:211–231.

Stepniewska I, Collins CE, Kaas JH (2005) Reappraisal of DL/V4 boundaries based on connectivity patterns of dorsolateral visual cortex in macaques. Cereb Cortex 15:809–822.

Tanaka M, Weber H, Creutzfeldt OD (1986) Visual properties and spatial distribution of neurones in the visual association area on the prelunate gyrus of the awake monkey. Exp Brain Res 65:11–37.

Tootell RB, Switkes E, Silverman MS, Hamilton SL (1988) Functional anatomy of macaque striate cortex. II. Retinotopic organization. J Neurosci 8:1531–1568.

Van Essen DC, Zeki SM (1978) The topographic organization of rhesus monkey prestriate cortex. J. Physiol 277:193–226.

Van Essen DC, Newsome WT, Maunsell HR (1984) The visual field representation in striate cortex of the macaque monkey: asymmetries, anisotropies, and individual variability. Vision Res 24: 429–448.

Van Essen DC, Drury HA, Dickson J, Harwell J, Hanlon D, Anderson CH (2001) An integrated software suite for surface-based analyses of cerebral cortex. J Am Med Inform Assoc 8:443–459.